

## Control of Iron(III) Spin-State in the Model Complexes of Azide Hemoprotein by Porphycene, Corrphycene, and Hemiporphycene Macrocycles

Saburo Neya,\*<sup>†</sup> C. K. Chang,<sup>‡</sup> Daichi Okuno,<sup>§</sup> Tyuji Hoshino,<sup>†</sup> Masayuki Hata,<sup>†</sup> and Noriaki Funasaki<sup>||</sup>

Department of Physical Chemistry, Graduate School of Pharmaceutical Sciences, Chiba University, Inage-Yayoi, Chiba 263-8522, Japan, Department of Chemistry, Michigan State University, East Lansing, Michigan 48824-1322, Center for Integrative Bioscience, Okazaki National Institutes, Okazaki, Aichi 444-8585, Japan, and Department of Physical Chemistry, Kyoto Pharmaceutical University, Yamashina, Kyoto 607-8414, Japan

Received November 21, 2004

Spin states of the iron(III) complexes of porphyrin, porphycene, hemiporphycene, and corrphycene bearing both 1-methylimidazole and azide as axial ligands were analyzed with infrared (IR) spectroscopy at 20 °C. The IR stretching band of coordinating azide split into two peaks around 2047 and 2017  $\text{cm}^{-1}$  reflecting an equilibrium between the high- ( $S = 5/2$ ) and low- ( $S = 1/2$ ) spin states. The high-spin fraction changed over a 0–90% range among the macrocycles, demonstrating that the tetrapyrrole array is essential to control the equilibrium.

Axial ligand and porphyrin substituent affect the energy level of the 3d electrons of heme iron. The spin-state equilibrium between the  $S = 5/2$  and  $1/2$  states is frequently found in the six-coordinate azide ( $\text{N}_3^-$ ) complex of hemoproteins<sup>1</sup> and in the model heme systems<sup>2</sup> of bis(3-chloropyridinato)(octaethylporphyrinato)iron(III) and bis(azido)-(tetraphenylporphyrinato)iron(III). Ikeue et al.<sup>3</sup> recently revealed a novel type of equilibrium between the  $S = 1/2$  and  $3/2$  states for the saddle-shaped (porphyrinato)iron(III) derivatives. The ferric heme in heme oxygenase<sup>4</sup> is suggested to be a mixture of the  $S = 3/2$  and  $1/2$  states.

Model complexes for azide hemoprotein have been analyzed to evaluate the role of globin. We have reported the for-

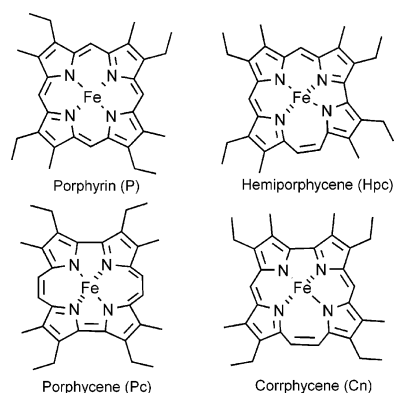


**Figure 1.** Structure of the Fe(III) complexes of etioporphyrin and the isomeric porphyrinoids. Axial ligand is omitted for clarity.

mation of a mixed-ligand complex, (protoporphyrinato)iron(III) $\text{N}_3^-$ OS(CH<sub>3</sub>)<sub>2</sub>, a model for catalase with the proximal tyrosinate, and suggested that the high-spin bias of the equilibrium in azide catalase comes from the coordination of the oxygen atom.<sup>5a</sup> We have also prepared a (protoporphyrinato)iron(III) coordinated with both  $\text{N}_3^-$  and 1-methylimidazole (1-MeIm)<sup>5b</sup> as a model for azide myoglobin (Mb), and found that the spin equilibrium profiles of the heme inside and outside of the protein matrix are quite similar. The crystal structure of (tetraphenylporphyrinato)iron(III) $\text{N}_3^-$ (1-MeIm) was resolved by Zhan et al.<sup>5c</sup> to provide the model coordination structure for azide Mb. All of these analyses were carried out for the iron atom placed in a square  $\text{N}_4$ -core formed by the four pyrrole rings of porphyrin (P).

Diverse variations of the coordination core of porphyrin are now feasible owing to the recent advances in the synthesis.<sup>6</sup> In porphycene (Pc), corrphycene (Cn), and hemiporphycene (Hpc), the  $\text{N}_4$ -core is rectangular, trapezoidal, and irregular quadrangle, respectively, as illustrated in Figure 1.

- (5) (a) Neya, S.; Morishima, I. *J. Am. Chem. Soc.* **1982**, *104*, 5658–5661. (b) Neya, S.; Hada, S.; Funasaki, N.; Umemura, J.; Takenaka, T. *Biochim. Biophys. Acta* **1985**, *827*, 157–163. (c) Zhang, Y.; Hallows, W. A.; Ryan, W. J.; Jones, J. G.; Carpenter, G. B.; Sweigart, D. A. *Inorg. Chem.* **1994**, *33*, 3306–3312.

\* To whom correspondence should be addressed. E-mail: sneya@p.chiba-u.ac.jp. Fax: +81-43-290-2925.

<sup>†</sup> Chiba University.

<sup>‡</sup> Michigan State University.

<sup>§</sup> Okazaki National Institutes.

<sup>||</sup> Kyoto Pharmaceutical University.

- (1) (a) Iizuka, T.; Yonetani, T. *Adv. Biophys.* **1970**, *1*, 157–182. (b) Scheidt, W. C.; Reed, C. A. *Chem. Rev.* **1981**, *81*, 543–555.  
 (2) (a) Scheidt, W. R.; Geiger, D. K.; Hayes, R. G.; Lang, G. *J. Am. Chem. Soc.* **1983**, *105*, 2625–2632. (b) Ellison, M. K.; Nasri, H.; Xia, Y.-M.; Marchon, J.-C.; Schulz, C. E.; Debrunner, P. G.; Scheidt, W. R. *Inorg. Chem.* **1997**, *36*, 4804–4811.  
 (3) (a) Ikeue, T.; Ohgo, Y.; Yamaguchi, T.; Takahashi, M.; Takeda, M.; Nakamura, M. *Angew. Chem., Int. Ed.* **2001**, *40*, 2617–2620. (b) Ikeue, T.; Ohgo, Y.; Ongay, O.; Vincente, M. G. H.; Nakamura, M. *Inorg. Chem.* **2003**, *42*, 5560–5571.  
 (4) Caignan, G. A.; Deshmukh, R.; Zeng, Y.; Wilks, A.; Bunce, R. A.; Rivera, M. *J. Am. Chem. Soc.* **2003**, *125*, 11842–11852.

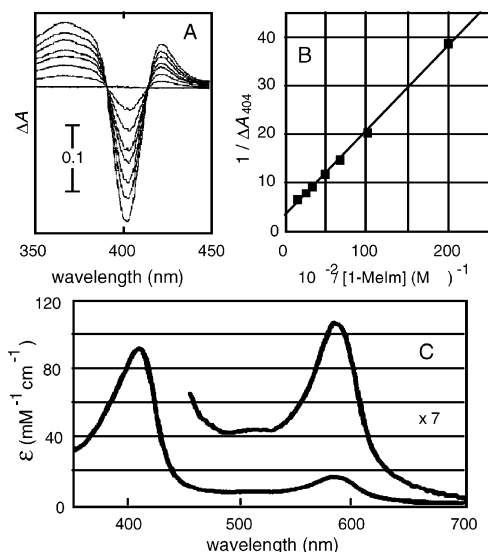
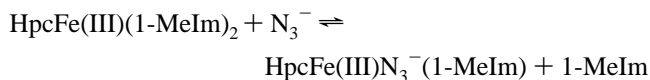


**Figure 2.** Formation of the mixed-ligand complex. (A) Soret absorption changes of 7  $\mu\text{M}$  HpcFe(III)(1-MeIm)<sub>2</sub> with addition of 0.5–6.0 mM NaN<sub>3</sub> in dimethyl sulfoxide at [1-MeIm] = 25 mM and 20 °C. (B) Analysis of the absorption decrease at 404 nm. (C) Calculated limiting spectrum for HpcFe(III)N<sub>3</sub><sup>-</sup>(1-MeIm).

These macrocycles provide a unique opportunity to perturb directly the equatorial ligand-field of heme iron. We report here the first IR investigation of molecular shape of porphyrinoids on the spin-state equilibrium of azide hemoprotein models. Since the heme in protein is apt to be deformed by globin,<sup>7</sup> the infrared (IR) band of the coordinating azide could monitor the globin effect.

Structures of etioporphyrin and the isomeric porphyrinoids<sup>8</sup> are shown in Figure 1. The five-coordinate iron(III) azide derivative, prepared from acid cleavage of the  $\mu$ -oxo-dimer in the presence of a saturating amount of aqueous sodium azide,<sup>9</sup> was purified on an alumina column with dichloromethane. Visible absorption spectra were recorded on a Shimadzu spectrophotometer. IR spectra at 2 cm<sup>-1</sup> resolution were measured on JASCO FT-IR spectrometer. Curve fitting was performed with Lorentzian function.

The six-coordinate iron(III) complex with N<sub>3</sub><sup>-</sup> and 1-MeIm as axial ligands was prepared by titrating sodium azide to the bis-1-MeIm species in dimethyl sulfoxide. Figure 2, part A, shows the Soret absorption changes of the hemiporphycene (Hpc) compound with clear isosbestic points at 391 and 415 nm. The transition was analyzed according to the following scheme:



The formation constant  $K = [\text{HpcFe(III)N}_3^-(1-\text{MeIm})][1-\text{MeIm}]/[\text{HpcFe(III)(1-MeIm)}_2][\text{N}_3^-] = 4.67 \pm 0.12$  (Figure 2, part B) of the mixed-ligand species was evaluated from the plots of  $(1/\Delta A, 1/[\text{N}_3^-])$  (Figure 2). The calculated limiting spectrum for HpcFe(III)N<sub>3</sub><sup>-</sup>(1-MeIm) in Figure 2 closely resembles that of the Mb containing HpcFe(III).<sup>10</sup> Spectrophotometric titrations for other macrocycles were similarly carried out, and the optical changes conformed to the above

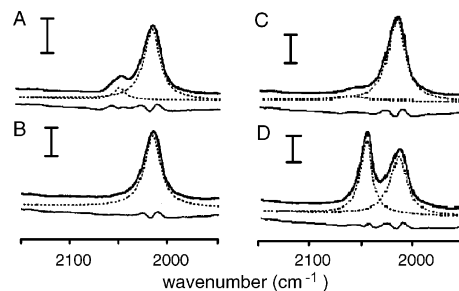


**Figure 3.** IR absorption spectra for the coordinating azide of mixed-ligand complex MFe(III)N<sub>3</sub><sup>-</sup>(1-MeIm) in chloroform at 20 °C. Macrocycle M is (A) P, (B) Pc, (C) Hpc, or (D) Cn. Broken curves represent the fitted bands. The small 2061-cm<sup>-1</sup> peak in C is from residual HpcFe(III)N<sub>3</sub><sup>-</sup>. The vertical scale stands for  $\Delta A = 0.01$ .

**Table 1.** Visible Absorption Spectra of MFe(III)N<sub>3</sub><sup>-</sup>(1-MeIm) in Dimethyl Sulfoxide at 20 °C and Mb

M <sup>a</sup>	$\lambda_{\text{max}}$ , nm ( $\epsilon$ , mM <sup>-1</sup> cm <sup>-1</sup> )				$K^b$
	406 (120)	528 (9.6)	562 (6.3)	615 (2.5)	
P	406 (120)	528 (9.6)	562 (6.3)	615 (2.5)	$9.4 \pm 0.2$
Pc	388 (103)	572 (18.4)	624 (49.5)		$3.3 \pm 0.1$
Hpc	406 (91)	510 (6.2)	580 (15.3)		$4.7 \pm 0.2$
Cn	418 (88)	521 (8.3)	638 (2.9)		$30.8 \pm 0.8$
Hpc-Mb <sup>c</sup>	409 (92)	510 (6.3)	580 (13.8)		

<sup>a</sup> M, macrocycle in Figure 1. <sup>b</sup> Formation constant of the mixed-ligand complex defined in the text. <sup>c</sup> Mb containing Hpc. See ref 10.

equilibrium scheme. The formation constants and limiting spectra are summarized in Table 1.

IR spectroscopy has been used to monitor the spin-state equilibrium in the azide complexes of hemes<sup>2b,5b</sup> and hemoproteins.<sup>12</sup> Figure 3 shows the absorption spectra for asymmetric stretching vibration modes of the iron-bound azide; the mixed-ligand complexes for the IR measurements were prepared after adding a stoichiometric amount of 1-MeIm to the five-coordinate azide iron(III). PFe(III)N<sub>3</sub><sup>-</sup>(1-MeIm) in part A exhibits two peaks at 2049 and 2016 cm<sup>-1</sup>. The peak positions are different from the 2060 cm<sup>-1</sup> band of the five-coordinate PFe(III)N<sub>3</sub><sup>-</sup> (result not shown), but similar to 2046 and 2023 cm<sup>-1</sup> of native Mb.<sup>12</sup>

The isomeric porphyrins caused remarkable IR changes. In the spectrum of CnFe(III)N<sub>3</sub><sup>-</sup>(1-MeIm) (Figure 3, part D),

- Sessler, J. L.; Gebauer, A.; Vogel, E. In *Porphyrin Handbook*; Kadish, K. M., Smith, K. M., Guillard, R., Eds.; Academic Press: San Diego, CA, 2000; Vol. 2, pp 1–54.
- Shelnett, J. A.; Song, X.-Z.; Ma, J.-G.; Jia, S.-L.; Jentzen, W.; Medforth, C. *Chem. Soc. Rev.* **1998**, 27, 31–41.
- (a) Fuhrhop, J.-H.; Smith, K. M. In *Porphyrins and Metalloporphyrins*; Smith, K. M., Ed.; Elsevier: Amsterdam, 1975; pp 765–766. (b) Vogel, E.; Balci, M.; Pramod, K.; Koch, P.; Lex, J.; Ermer, O. *Angew. Chem., Int. Ed. Engl.* **1987**, 26, 928–931. (c) Neya, S.; Nishinaga, K.; Ohyama, K.; Funasaki, N. *Tetrahedron Lett.* **1998**, 39, 5217–5220. (d) Vogel, E.; Bröring, M.; Weghorn, S. J.; Scholz, P.; Deponte, D.; Lex, J.; Schmickler, H.; Schaffner, K.; Braslavsky, S. E.; Müller, M.; Pörting, S.; Fowler, C. J.; Sessler, J. L. *Angew. Chem., Int. Ed. Engl.* **1997**, 36, 1651–1654.
- Maricondi, C.; Swift, W.; Straub, D. K. *J. Am. Chem. Soc.* **1969**, 91, 5205–5210.
- Optical titration of sodium azide to the Mb reconstituted with HpcFe(III)<sup>11</sup> afforded a binding constant  $4.3 \times 10^4 \text{ M}^{-1}$  in 0.1 M Tris at pH 7.0 and 20 °C. The visible spectrum is provided in Table 1.
- Neya, S.; Tsubaki, M.; Hori, H.; Yonetani, T.; Funasaki, N. *Inorg. Chem.* **2001**, 40, 1220–1225.
- (a) McCoy, S.; Caughey, W. S. *Biochemistry* **1970**, 9, 2387–2393. (b) Alben, J. O.; Fajer, L. Y. *Biochemistry* **1972**, 11, 842–847. (c) Bogumil, R.; Hunter, C. L.; Maurus, R.; Tang, H.-L.; Lee, H.; Lloyd, E.; Brayer, G. D.; Smith, M.; Mauk, A. G. *Biochemistry* **1994**, 33, 7600–7608.

**Table 2.** Position (Half-Height Width) of the Azide Stretching Bands in  $\text{cm}^{-1}$  for  $\text{MFe(III)N}_3^-(1\text{-MeIm})$  and Mb

M <sup>a</sup>	high-spin	low-spin	$K_s^b$	ref
P	2049 (13)	2017 (19)	10/90	this work
Pc		2017 (19)	0	this work
Hpc		2017 (19)	0	this work
Cn	2048 (14)	2016 (19)	52/48	this work
Cn <sup>c</sup>	2046 (15)	2020 (18)	92/8	11
Mb	2046 (8)	2023 (9–10)	11/89	12b

<sup>a</sup> M, macrocycle in Figure 1. <sup>b</sup>  $K_s = [\text{high spin}]/[\text{low spin}]$  as calculated from the intensity ratio of the two azide bands. <sup>c</sup> Di(ethoxycarbonyl)-Cn.

the two signals appeared at 2048 and 2016  $\text{cm}^{-1}$ . The band positions are almost identical with those found in  $\text{PFe(III)N}_3^-(1\text{-MeIm})$  in part A. However, the two peaks in  $\text{CnFe(III)N}_3^-(1\text{-MeIm})$  have almost the same intensities. The 2048- $\text{cm}^{-1}$  band of  $\text{CnFe(III)N}_3^-(1\text{-MeIm})$  is more intense as compared with the corresponding peak in  $\text{PFe(III)N}_3^-(1\text{-MeIm})$ . The Pc and Hpc macrocycles also caused an anomaly.  $\text{HpcFe(III)N}_3^-(1\text{-MeIm})$  in part C and  $\text{PcFe(III)N}_3^-(1\text{-MeIm})$  in part B exhibit single peaks at 2017  $\text{cm}^{-1}$  without an additional signal around 2048  $\text{cm}^{-1}$ . These IR results are compiled in Table 2.

The appearance of the two IR bands from the azide in the porphyrin complex  $\text{PFe(III)N}_3^-(1\text{-MeIm})$  demonstrates that the iron(III) atom is in an equilibrium between the  $S = 1/2$  and  $5/2$  states. On the basis of the reported results,<sup>5b,12</sup> we assigned the two bands around 2017 and 2048  $\text{cm}^{-1}$  in Figure 3 to the low-spin and high-spin forms, respectively. The spin equilibrium constant  $K_s = [\text{high spin}]/[\text{low spin}]$  in Table 2 was estimated from the integrated intensity ratio of the two bands because the extinction coefficients of these peaks are essentially the same.<sup>12</sup> Table 2 shows that high spin fraction varies over a 0–92% range. Consistent results were obtained from the magnetic moment with the Evans method.<sup>13</sup>

It is notable that  $\text{PcFe(III)N}_3^-(1\text{-MeIm})$  exhibits a single IR band at 2017  $\text{cm}^{-1}$ . The result suggests a pure low-spin state for  $\text{PcFe(III)N}_3^-(1\text{-MeIm})$ , in contrast with  $\text{PFe(III)N}_3^-(1\text{-MeIm})$  that exhibits spin equilibrium. According to X-ray analysis, the  $\text{N}_4$ -core in Pc (7.647  $\text{\AA}^2$ )<sup>6</sup> is narrower than that in P (8.503  $\text{\AA}^2$ ).<sup>6</sup> The core contraction in Pc results in a shorter Fe–N(pyrrole) bond and stronger equatorial ligand-field of the iron. A stronger equatorial field subsequently raises the energy level of the  $3d_{x^2-y^2}$  orbital to destabilize the high-spin electron configuration. It is thus likely that the narrower  $\text{N}_4$ -core of Pc induces a pure low-spin state for  $\text{PcFe(III)N}_3^-(1\text{-MeIm})$ .  $\text{HpcFe(III)N}_3^-(1\text{-MeIm})$  also exhibits a single IR band at 2017  $\text{cm}^{-1}$  to indicate a pure low-spin

state as well. Although the  $\text{N}_4$ -core of Hpc is larger (8.246  $\text{\AA}^2$ )<sup>7d</sup> than that of Pc (7.647  $\text{\AA}^2$ ),<sup>6</sup> the Hpc core is still slightly smaller than the P core (8.503  $\text{\AA}^2$ ).<sup>6</sup> The slight but appreciable core contraction in Hpc seems sufficient to tip completely the equilibrium toward the low spin.

The IR analysis reveals another intriguing result for the Cn complex. Table 2 shows that  $\text{CnFe(III)N}_3^-(1\text{-MeIm})$  is in spin equilibrium like  $\text{PFe(III)N}_3^-(1\text{-MeIm})$ . However, the high-spin fraction 52% in the Cn complex is significantly larger than 10% in the P derivative. The  $\text{N}_4$ -cavity area<sup>12</sup> of Cn, 8.273  $\text{\AA}^2$ , is almost identical with 8.246  $\text{\AA}^2$  of Hpc.<sup>7d</sup> Despite their comparable core sizes,  $\text{CnFe(III)N}_3^-(1\text{-MeIm})$  is much more high-spin. What is the origin of this difference? From the structures of Cn, it is evident that two of the four N(pyrrole)–Fe–N(pyrrole) bond angles in  $\text{CnFe(III)Cl}$ , i.e., 74° and 104°,<sup>14a</sup> deviate significantly from 90°. Such a large angular distortion is not found in the Hpc macrocycle.<sup>15</sup> Deviation from the orthogonality for the Fe–N(pyrrole) bonds in Cn tends to destabilize the in-plane configuration of iron atom.<sup>16,17</sup> This is consistent with the observation that the formation constant of the mixed-ligand complex of Cn is 1 order of magnitude larger than that of other macrocycles (Table 1). This observation may be interpreted to indicate the iron is more easily displaced by azide from the aromatic plane. It is thus likely that the high-spin bias in  $\text{CnFe(III)N}_3^-(1\text{-MeIm})$  is caused by the trapezoidal  $\text{N}_4$ -core which facilitates out-of-plane displacement of the iron atom.

We have already reported a 92% high-spin population for another  $\text{CnFe(III)N}_3^-(1\text{-MeIm})$ <sup>11</sup> bearing di(ethoxycarbonyl) substituents. The high-spin content 52% in the present etio- $\text{CnFe(III)N}_3^-(1\text{-MeIm})$  is smaller than the 92% found in di(ethoxycarbonyl) $\text{CnFe(III)N}_3^-(1\text{-MeIm})$ .<sup>11</sup> The strongly electron-withdrawing ethoxycarbonyl groups place more positive charge on the central iron and increase its charge attraction to axial azide. Removal of the ester side chains could weaken the axial ligand field and shift the spin equilibrium to high spin. Thus, etio- $\text{CnFe(III)N}_3^-(1\text{-MeIm})$  is expected to have a larger high-spin fraction than di(ethoxycarbonyl)- $\text{CnFe(III)N}_3^-(1\text{-MeIm})$  does. However, etio- $\text{CnFe(III)N}_3^-(1\text{-MeIm})$  is actually more low-spin, as shown in Table 2. The unexpected result suggests participation of a factor other than the inductive effect of the ester groups. A structural comparison between the two  $\text{CnFe(III)I}$  complexes indicates that the etio-Cn compound has a smaller  $\text{N}_4$ -core (7.897  $\text{\AA}^2$ )<sup>14</sup> than the di(ethoxycarbonyl)-Cn derivative (8.015  $\text{\AA}^2$ ).<sup>18</sup> Thus, an increase in the low-spin fraction of the etio-Cn complex is interpreted to reflect the core contraction that exceeds electron withdrawal by the ester substituents.

In summary, our IR analysis disclosed that the spin-state of the six-coordinate azide heme is a function of the  $\text{N}_4$ -core geometry, demonstrating that iron-bound azide is a promising probe to evaluate the subtle deformations<sup>7</sup> in heme by the protein matrix.

**Acknowledgment.** We are indebted to Dr. Yoshiki Ohgo and Professor Mikio Nakamura, Toho University School of Medicine, for the magnetic moment measurement.

IC048353C

- (13) Magnetic moments of the  $\text{MFe(III)N}_3^-(1\text{-MeIm})$  complexes, as estimated with the Evans method in dichloromethane at 25 °C, are 2.6 (P), 2.0 (Pc), 1.9 (Hpc), and 3.3 (Cn)  $\pm 0.1 \mu_B$ , corresponding to the high-spin fractions of 20%, 6%, 4%, and 37%, respectively.
- (14) (a) Ohgo, Y.; Neya, S.; Ikeue, T.; Takahashi, M.; Takeda, M.; Funasaki, N.; Nakamura, M. *Inorg. Chem.* **2002**, *41*, 4627–4629. (b) Rachlewicz, K.; Latos-Grazynski, L.; Vogel, E.; Ciunik, Z.; Jerzykiewicz, L. B. *Inorg. Chem.* **2002**, *41*, 1979–1988.
- (15) Ohgo, Y.; Neya, S.; Takahashi, M.; Takeda, M.; Funasaki, N.; Nakamura, M. *Chem. Lett.* **2003**, *32*, 526–527.
- (16) Neya, S.; Imai, K.; Hori, H.; Ishikawa, H.; Ishimori, K.; Okuno, D.; Nagatomo, S.; Hoshino, T.; Hata, M.; Funasaki, N. *Inorg. Chem.* **2003**, *42*, 1456–1461.
- (17) Neya, S.; Hoshino, T.; Hata, M.; Funasaki, N. *Chem. Lett.* **2004**, *33*, 114–115.
- (18) Ohgo, Y.; Neya, S.; Funasaki, N.; Nakamura, M. *Acta Crystallogr.* **2001**, *C57*, 694–695.